Green Chemistry

Accepted Manuscript

ROYAL SOCIETY OF CHEMISTRY

www.rsc.org/greenchem

Green Chemistry

RSCPublishing

COMMUNICATION

Hydroxyapatite, an exceptional catalyst for the gas-phase deoxygenation of bio-oil by aldol condensation

Cite this: DOI: 10.1039/xoxxoooooox

Received ooth January 2014,
Accepted ooth January 2014

DOI: 10.1039/xoxxoooooox

www.rsc.org/

E. G. Rodrigues, T. C. Keller, S. Mitchell and J. Pérez-Ramírez*

Hydroxyapatites with high surface concentrations of calcium exhibit outstanding activity, selectivity, and stability in the gas-phase condensation of propanal in comparison with well-established base catalysts. These abundant and low-cost materials can be attractively used for the deoxygenation of bio-oil, contributing to the sustainable manufacture of renewable second-generation bio-fuels.

The production of second-generation biofuels from pyrolysis oil comprises an intermediate solution for the partial substitution of existing fossil-based feedstocks.[1] A major current challenge involves the development of efficient routes to reduce the high oxygen content of the crude bio-oil (*e.g.* 10-50 wt.%), which impedes its direct application in modern combustion engines due to the associated low heating value, chemical instability, and corrosiveness.[2] Although the required specifications can be met through conventional hydrodeoxygenation, this approach is impractical due to the excessive consumption of expensive hydrogen.[3] Alternatively, the deoxygenation of intrinsically reactive bio-oil constituents can be attractively exploited through intermediate upgrading treatments to decrease the subsequent hydrogen demand, while simultaneously converting lower-boiling points fractions into gasoline-range molecules.[4] In particular, aldol condensations draw attention due to the large aldehyde fraction of bio-oil (up to 20 wt.%). This class of reaction can be catalysed by solid bases such as alkali-metal containing zeolites,[5] alkaline-earth metal oxides,[6] hydrotalcites,[7] and alkaline activated high-silica zeolites.[8] Herein, the deactivation due to blockage of the active sites by heavy oligomers can be minimised by moderation of the basic strength.[6]

Calcium hydroxyapatite (HA), a well-known mineral, has attracted continued interest as a catalyst or catalyst support since it can be synthesised with a tuneable number of acid and base sites by varying the composition.[9] The compositional flexibility arises from the possible loss and/or substitution of the calcium or phosphate ions, which in stoichiometric form has a molar Ca/P ratio of 1.67 ($Ca_{10}(PO_4)_6(OH)_2$, **Fig. 1a**). While in Ca-deficient forms the consequent charge imbalance is corrected by the introduction of H^+ and the partial substitution of OH^- by H_2O,[10-11] it was hypothesised that Ca-rich HA (Ca/P > 1.67) could comprise a mixture of the stoichiometric HA and $Ca(OH)_2$ or solid solutions resulting upon the replacement of tetrahedral PO_4^{3-} by CO_3^{2-} ions.[12] The acid-base character of HA yields unique catalytic performance in the self-coupling of ethanol to produce biogasoline (Guerbet reaction), which was shown to depend on the calcium content and correspondingly to the density of basic sites.[13] However, in relation to aldol-type condensations the effectiveness of

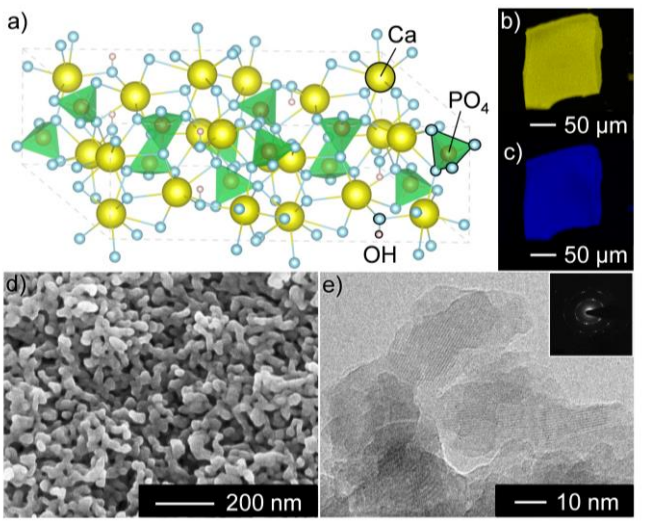

Fig. 1 (a) Atomic structural representation, EDX maps evidencing the macroscopic distribution of (b) calcium and (c) phosphorus, (d) SEM and (e) TEM micrographs of the particle and crystal morphology, and (e, inset) selected area electron diffraction pattern of the stoichiometric HA.

calcium hydroxyapatite catalysts have only been studied for liquid-phase applications in fine-chemical synthesis.[14] Comprising non-toxic, earth-abundant elements, and attainable *via* affordable, energy-efficient routes, these materials presents ideal qualities as catalysts for the sustainable refining of bio-oil.

This work reports the outstanding performance of HA in the self-condensation of propanal, a common light-aldehyde constituent of bio-oil (**Scheme 1**). HAs of distinct composition

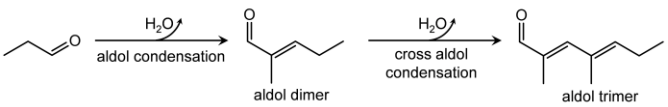

Scheme 1 Reaction pathway of the base-catalysed self-condensation of propanal.

were attained by varying the nominal Ca/P ratio (1-2) during the aqueous precipitation of diammonium phosphate in calcium nitrate at room temperature and constant pH (9.5), followed by drying and calcination at 600°C. Full details of the synthesis protocol are available in the ESI. The properties of the fresh catalysts, which are coded according to the bulk composition of the resulting sample (**Table 1**), are typical of those expected for solids precipitated under these conditions.[9] HA was identified as the only crystalline product (**Fig. 2a** and **Fig. S1**; reference data JCPDS #73-1731) and the highest crystallinity was observed for the sample matching the stoichiometric composition. Consistently, the skeletal density evidenced by He pycnometry (3.02 g cm^{-3} for HA-1.49 and HA-1.69, 3.04 g cm^{-3} for HA-1.67) was close to the theoretical value (3.08 cm^3 g^{-1}).[10] In agreement with previous studies,[15] chemical analyses revealed that the bulk molar ratios of Ca/P (1.5-1.7) fell within a much narrower range than the values applied during synthesis. Furthermore, although showing a similar tendency to the bulk, the surface (1.02-1.23) was found to be considerably calcium deficient (**Table 1**). The homogeneous macroscopic distribution of calcium and phosphorus was confirmed by energy dispersive X-ray (EDX) spectroscopy (**Fig. 1b,c** and **Fig. S1**). Further examination by scanning and transmission electron microscopy (**Fig. 1d,e** and **Fig. S2**), reveals that the HA catalysts comprise large mesoporous agglomerates of loosely-packed nanocrystals (10-40 nm). Correspondingly, the materials exhibit similar specific surface areas (S_{BET}, **Table 1**) and mesopore volumes (*ca.* 0.40 cm^3 g^{-1}), the latter originating from mesopores of *ca.* 10-30 nm in diameter (**Fig. S3**).

The basicity of the HAs was evaluated by the temperature-programmed desorption (TPD) of carbon dioxide (**Fig. 2b**). As expected, the total amount of CO_2 evolved increases with the Ca/P ratio and the temperature of desorption varies. In particular, while the Ca-deficient materials only exhibit a low concentration of weak sites, corresponding to the desorption at 140°C, the stoichiometric material also displays a broad peak at *ca.* 300°C, whereas a third site of intermediate strength is observed for the Ca-rich samples. This highlights the close association between the surface concentration of Ca^{2+} and the increased density and strength distribution of basic sites. To provide further insight into the nature of the basic sites, *in situ* DRIFT spectra of adsorbed CO_2 were recorded over the catalysts at different temperature (**Fig. S4**). All samples exhibited a band at 1375 cm^{-1}, which was assigned to the formation of surface (PO_x)-carbonate species.[16] The disappearance of this band in the HA-1.49 sample at 200°C suggests that the weak basic sites observed in the CO_2-TPD profiles correspond to surface O^{2-} ions belonging to phosphate groups. On the other hand, the distinct contributions observed

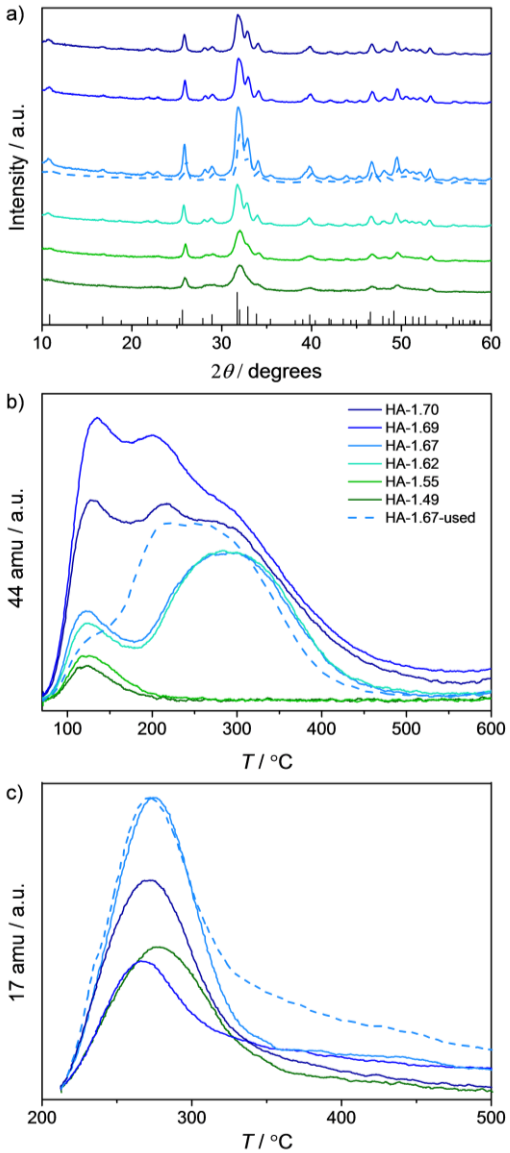

Fig. 2 (a) X-ray diffraction patterns with reference vertical lines indicated, (b) CO_2-TPD profiles, and (c) NH_3-TPD profiles of the hydroxyapatite catalysts. The colour code depicted in (b) applies to (a) and (c).

between 1760-1590 cm^{-1} pertain to hydrogenocarbonate species in different local configurations.[16] Accordingly, the CO_2 evolved at higher temperatures can predominantly be linked to the reaction of CO_2 with basic OH^- groups ($CO_2 + 2OH^- \rightarrow CO_3^{2-} + H_2O$). The increased contribution in the order: HA-1.49 > HA-1.67 > HA-1.69, is in good agreement with the higher amount of CO_2 evolved in samples with the respective

calcium contents, since this directly relates to the concentration of OH^- species present. However, the specific assignment of the higher temperature desorption peaks observed by CO_2-TPD is not yet fully clear. The acid properties were assessed by NH_3-TPD and the infrared study of adsorbed pyridine (**Figs. 2c** and **Fig. S5**). In this case, all of the hydroxyapatites display a single broad desorption centred at 270°C in the NH_3-TPD profiles, the intensity of which reaches a maximum in the stoichiometric sample. The analysis of adsorbed pyridine confirmed the Lewis-acidic nature of the acid sites (**Fig. S5**),[17] and the higher concentration in the HA-1.67 catalyst. Moreover analysis of the amount adsorbed at increasing temperatures evidences a slightly higher strength with respect to the Ca-rich and Ca-deficient samples (**Table 1** and **Fig. S5**).

The performance of the HA catalysts was assessed in the aldol condensation of propanal at 400°C (weight hourly space velocity = 9.72 h^{-1}) to reflect the operating temperature of a pyrolysis outlet stream. While all of the samples effectively catalysed the C–C bond formation, the activity and selectivity depended markedly on the catalyst composition (**Fig. 3a**). Specifically, the propanal conversion almost doubled as the bulk Ca/P ratio increased from 1.49 to 1.62, above which it reached a maximum. The increased activity correlated with the evolution of the trimer selectivity, which also reaches a maximum (over 30%) over the calcium-rich samples. The latter attain an impressive performance, exhibiting conversion rates of nearly 100 $mmol_{propanal}$ h^{-1} $g_{catalyst}^{-1}$, which could be ascribed to the increased amount of weak basic sites and/or to the simultaneous presence of sites with higher strength when compared with the Ca-deficient catalysts.

The potential of HAs was benchmarked to well-established base catalysts, namely a nanocrystalline MgO (coded'MgO_{nano}', S_{BET} = 770 m^2 g^{-1}), an activated high surface area Mg-Al hydrotalcite (coded 'HT_a', molar Mg/Al = 3, S_{BET} = 177 m^2 g^{-1}) and a caesium-exchanged zeolite X (coded 'CsX', S_{BET} = 365 m^2 g^{-1}). In addition, to assess the possible contribution of a phase-separated calcium hydroxide to the superior activity of Ca-rich HAs, the performance of bulk $Ca(OH)_2$ (S_{BET} = 17 m^2 g^{-1}) and CaO (S_{BET} = 24 m^2 g^{-1}) were also investigated. Comparatively, these materials display quite distinct relative basicity, which based on our experimental analysis (**Figs. 2b** and **S6**) and on literature expectations can be ordered in terms of strength as: $Ca(OH)_2$/CaO > MgO[18] > HT ≈ HA > CsX. However, none of the reference materials display a remotely close initial rate of conversion (**Fig. 3b**) or a as high selectivity to the aldol-condensation products (**Table S1**) as

Table 1 Characterisation data of the catalysts

Sample	Ca/P mol mol^{-1}			S_{BET} / m^2 g^{-1}	c_L[c] / μmol_{Py} g^{-1}
	nominal	bulk[a]	surface[b]		
HA-1.49	1.00	1.49	1.02	45	47
HA-1.55	1.50	1.55	-	57	-
HA-1.62	1.64	1.62	-	59	-
HA-1.67	1.67	1.67	1.26	63 (41)[d]	82
HA-1.70	1.70	1.70	-	65	-
HA-1.69	2.00	1.69	1.23	73	69

[a]Determined in the solids by inductively coupled plasma optical emission spectroscopy. [b]Determined by X-ray photoelectron spectroscopy. [c]Concentration of Lewis acid sites derived from the IR study of adsorbed pyridine (Py) indicated for comparative purposes. [d]Used sample after calcination at 600ºC.

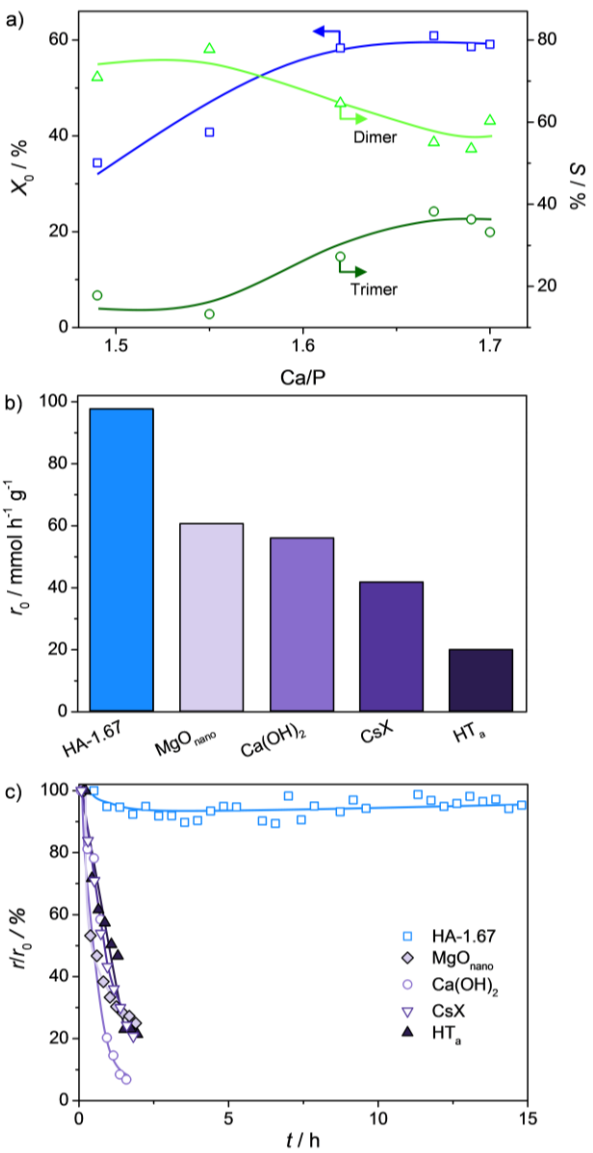

Fig. 3 (a) Influence of the bulk molar Ca/P ratio on the conversion of propanal and the selectivity to the dimer and trimer products over the HA catalysts, (b) initial rate and (c) percentage of the initial activity *versus* time-on-stream for the HA-1.67 material and traditional base catalysts. Reaction conditions: 0.1 g catalyst, 400°C, WHSV = 9.72 h^{-1}, 50 cm^3 min^{-1} He flow.

HA-1.67. Furthermore, in contrast to the stable performance of the latter, which retained over 90% of its initial activity even after 15 h, the state-of-the-art catalysts all deactivated to less than 20% of the initial rate within 2.5 h on stream (**Fig. 3c**). Consistent with these observations, analysis of the used catalysts by thermogravimetry revealed the deposition of larger amounts of coke over the MgO_{nano}, HT_a, and CsX catalysts (9, 6, and 11%, respectively) with respect to HA-1.67 (2%). On the other hand, the deactivation of the highly basic $Ca(OH)_2$ and CaO catalysts can be related to their complete bulk carbonation under the reaction conditions, which explains the 40% weight loss observed at 700°C by thermogravimetry (**Fig. S7**).[19] The high-temperature carbonation of these materials indicates that the superior performance of the Ca-rich HA catalysts is not likely to be due to the presence of phase-separated CaO and/or $Ca(OH)_2$, since this contribution is not present in the HAPs profiles. No major structural alterations were evidenced upon calcination of the used HA-1.67 catalyst at 600°C to remove deposited coke species. A slight reduction in the crystallinity and surface area, coupled with an increased concentration of basic sites of intermediate strength indicate the occurrence of some structural rearrangement during the reaction. Nonetheless, the properties remain comparable to the HA catalysts of higher bulk Ca/P ratio, and a similar activity was attained upon subsequent reapplication.

Despite the similar trends evidenced by CO_2-TPD, the basicity of the HT_a does not originate a comparable activity to the HA-1.67 catalyst. Consequently, besides the strength, the inherent nature of the basic sites in HA, associated with the presence of Ca^{2+} at the crystal surface appears to be the key to their exceptional behaviour. Nevertheless, it is unclear which of the basic sites evidenced by CO_2-TPD in the hydroxyapatites is active. Alternatively, while the Lewis acidity does not appear to have a critical impact, a possible cooperative role between acid and base sites[6,20] cannot be excluded as the basis of the superior performance of the HA catalysts. These essential aspects clearly merit more-detailed future study. Furthermore, opportunities to extend the scope of HA catalysts, for example by tuning the acid-base properties though ionic substitution of the cationic Ca position (Sr, Mg, *etc.*), or the anionic PO_4^{3-} (CO_3^{2-}, HPO_4^{2-}), or OH^- (CO_3^{2-}, F^-) positions or by controlling the crystal morphology, deserve immediate exploration.

Conclusions

Calcium hydroxyapatites have been demonstrated as highly efficient aldol condensation catalysts, exhibiting significantly higher (over 50%) and much more stable reaction rates than other key classes of base catalyst, with enhanced selectivity to the dimeric and trimeric products. This exceptional behaviour is attributed to the combination between the intrinsic strength and nature of the basic sites, the density of which is increased in the stoichiometric and calcium-rich forms in agreement with a higher surface concentration of calcium. In view of their availability and competitiveness, HAs stand out as attractive candidates for the intermediate catalytic deoxygenation of bio-oil prior to hydrotreatment.

Acknowledgements

Financial support by the European Union Seventh Framework Programme (FP7/2007-2013, grant 604307) and by ETH Zurich (grant ETH-31 13-1) is acknowledged. The authors thank Dr. D. Siewert (LMN PSI) and Dr. I. Czekaj (ETH Zurich) for XPS analyses. Scientific Center for Optical and Electron Microscopy (ScopeM) at ETH Zurich is thanked for use of its facilities.

Notes and references

[a] *Institute for Chemical and Bioengineering, Department of Chemistry and Applied Biosciences, ETH Zurich, Vladimir-Prelog-Weg 1, CH-8093 Zurich, Switzerland.*
E-mail: jpr@chem.ethz.ch; Fax: +41 44 6331405; Tel: +41 44 6337120.

Electronic Supplementary Information (ESI) available: Detailed experimental procedure and additional characterisation data. See DOI: 10.1039/c000000x/

1 (a) S. Czernik, A.V. Bridgwater, *Energy Fuels*, 2004, **18**, 590; (b) G.W. Huber, A. Corma, *Angew. Chem. Int. Ed.*, 2007, **46**, 7184; c) M. Stöcker, *Angew. Chem. Int. Ed.*, 2008, **47**, 9200.

2 (a) Z. Qi, C. Jie, W. Tiejun, X. Ying, *Energy Convers. Manage.*, 2008, **48**, 87; (b) P.M. Mortensen, J.-D. Grunwaldt, P.A. Jensen, K.G. Knudsen, A.D. Jensen, *Appl. Catal. A*, 2001, **407**, 1; (c) I. Graça, J.M. Lopes, H.S. Cerqueira, M.F. Ribeiro, *Ind. Eng. Chem. Res.*, 2013, **52**, 275.

3 (a) A. Corma, G.W. Huber, L. Sauvanaud, P. O'Connor, *J. Catal.*, 2007, **247**, 307; (b) I. Graça, F. Ramô Ribeiro, H.S. Cerqueira, Y.L. Lam, M.B.B. de Almeida, *Appl. Catal. B*, 2009, **90**, 556; (c) E. Furimsky, *Appl. Catal. A*, 2000, **199**, 147; (d) T.P. Vispute, H. Zhang, A. Sanna, R. Xia, G.W. Huber, *Science*, 2012, **330**, 1222.

4 (a) A.H. Zacher, M.V. Olarte, D.M. Santosa, D.C. Elliott, S.B. Jones, *Green Chem.*, 2014, **16**, 491; (b) D. D. Hsu, *Biomass Bioenergy*, 2012, **45**, 41; (c) P. Tu Nguyet, D. Shi, D.E. Resasco, *Appl. Catal. B*, 2014, **145**, 10; (d) T.N. Pham, T. Sooknoi, S.P. Crossley, D.E. Resasco, *ACS Catal.*, 2013, **3**, 2456.

5 M.J. Climent, A. Corma, S.B.A. Hamid, S. Iborra, M. Mifsud, *Green Chem.*, 2006, **8**, 524.

6 (a) H. Tsuji, F. Yagi, H. Hattori, H. Kita, *J. Catal.*, 1994, *148*, 759-770; (b) W. Shen, A.A. Tompsett, R. Xing, W.C. Conner, G.W. Huber, *J. Catal.*, 2012, **286**, 248.

7 S. Abelló, F. Medina, D. Tichit, J. Pérez-Ramírez, J.C. Groen, J.E. Sueiras, P. Salagre, Y. Cesteros, *Chem. Eur. J.*, 2005, **11**, 728.

8 T.C. Keller, E.G. Rodrigues, J. Pérez-Ramírez, *ChemSusChem*, 2014, **7**, 1729.

9 (a) F.-Z. Su, J. Ni, Y. Cao, H.-Y. He, and K.-N. Fan, *Angew. Chem. Int. Ed.*, 2009, **48**, 4390; (b) V.C. Ghantani, S.T. Lomate, M.K. Dongare, S.B. Umbarkar, *Green Chem.*, 2013, **15**, 1211.

10 J.O. Nriagu, P.B. Moore, in: *Phosphate minerals*, Springer-Verlag, Berlin, 1984, p. 330.

11 S.J. Joris and C.H. Amberg, *J. Phys. Chem.*, 1971, **75**, 3167.

12 (a) G. Bonel, J.C. Heughebaert, J.L. Lacout, A. Lebugle, Ann. NY Acad. Sci., 1988, **115**; (b) J.C. Elliot, in*: Studies in Inorganic Chemistry*, Vol.18, Elsevier, Amsterdam, 1994, p. 114; (c)

M. Vignoles, G. Bonel, D.W. Holcomb, R.A. Young, *Calcified Tissue Int.*, 1988, **43**, 33.

13 J.T. Kozlowski, R.J. Davis, *ACS Catal.*, 2013, **3**, 1588.

14 (a) S. Sebti, R. Tahir, R. Nazih, A. Saber, S. Boulaajaj, *Appl. Catal. A*, 2002, **228**, 155; (b) M. Subramanian, G. Vanangamudi, G. Thirunarayanan, *Spectrochim. Acta A*, 2013, **110**, 116; (c) S. Mallouk, K. Bougrin, A. Laghzizil, R. Benhida, *Molecules*, 2010, **15**, 813.

15 (a) T. Tsuchida, J. Kubo, T. Yoshioka, S. Sakuma, T. Takeguchi, W. Ueda, *J. Catal.*, 2008, **259**, 183; (b) M. Yoshinari, Y. Ohtsuka, T. Derand, *Biomaterials*, 1994, **15**, 529.

16 (a) S. Diallo-Garcia, M.B. Osman, J.-M. Krafft, S. Casale, C. Thomas, J. Kubo, G. Costentin, *J. Phys. Chem. C*, 2014, **118**, 12744; (b) Z.H. Cheng, A. Yasukawa, K. Kandori, T. Ishikawa, *J. Chem. Soc., Faraday Trans.*, 1998, **94**, 1501.

17 D. Stošić, S. Bennici, S. Sirotin, C. Calais, J.-L. Couturier, J.-L. Dubois, A. Travert, A. Auroux, *Appl. Catal. A*, 2012, **447-448**, 124.

18 Y. Yanagisawa, K. Takaoka, S. Yamabe, *J. Phys. Chem.*, 1995, **99**, 3704.

19 Y. Tang, J. Xu, X. Gu, *J. Chem. Sci.*, 2013, **125**, 313.

20 (a) M.J. Climent, A. Corma, S. Iborra, A. Velty, *J. Mol. Catal. A*, 2002, **182-183**, 327; (b) R.K. Zeidan, M. Davis, *J. Catal.*, 2007, **247**, 379, c) J. Tai, R.J. Davis, *Catal. Today*, 2007, **123**, 42.

Table of Contents graphic

Hydroxyapatite, an exceptional catalyst for the gas-phase deoxygenation of bio-oil by aldol condensation

Elodie G. Rodrigues, Tobias C. Keller, Sharon Mitchell and Javier Pérez-Ramírez*

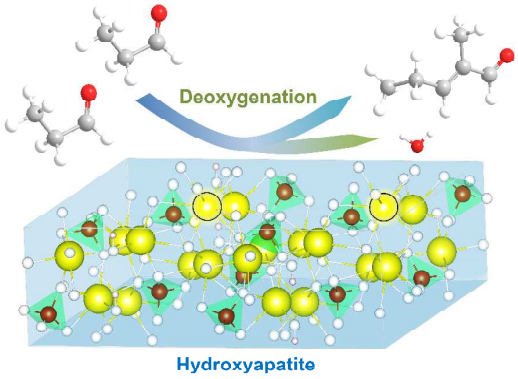

Hydroxyapatites displaying high surface concentrations of calcium exhibit exceptional performance in the gas-phase condensation of propanal, a model substrate for the intermediate deoxygenation of biocrude.